# Modelling of BLDCM with a double 3-phase stator winding and back EMF harmonics

**PIOTR DROZDOWSKI**

*Cracow University of Technology*
*Faculty of Electrical and Computer Engineering*
*Institute of Electromechanical Energy Conversion*
*ul. Warszawska 24, 31-155 Kraków, Poland*
*e-mail: pdrozdow@pk.edu.pl, xpiotrd@wp.pl*

**Abstract:** In this paper the mathematical model of the brushless DC motor (BLDCM) with a double 3-phase stator winding is analysed. Both the 3-phase windings are mutually displaced by 30 electrical degree. Special care has been sacrificed to influence of higher harmonics of induced electromotive forces (EMF) on electromagnetic torque and zero sequence voltages that may be used for sensorless control. The mathematical model has been presented in natural variables and, after transformation to symmetrical components, in a vector form. This allows, from one side, for formulating the equivalent circuit suitable for circuit oriented simulators (e.g.: Spice, SimPowerSystems of Simulink) and, from the other point of view, for analysis of higher harmonics influence on control possibilities. These considerations have been illustrated with some results of four quadrant operation obtainded due to simulation at automatic control.

**Key words:** brushless dc motor, double stator winding, harmonics of back EMF

## 1. Introduction

The brushless direct current motors (BLDCM) can be controlled using voltage or current control [4, 16, 17, 19]. The voltage control forces voltages supplying the motor. This can be performed in the input of the electronic commutator using external power electronics device, e.g. a dc switching regulator or inside the commutator. The commutator can operate under the 3-phase control mode or the 2-phase mode. During the current control the commutator becomes the multi-phase current source forcing sinusoidal 3-phase currents or rectangular 2-phase currents [4, 5, 14]. The current control can be also performed using a current source inverter as the commutator [5, 6, 10]. For all the control methods various sensorless modes of rotor field position determination can be applied [11, 12, 16, 19].

In this paper the BLDCM with a double stator winding is analysed. This motor has two 3-phase windings displaced each other with 30 electrical degrees. For the control all the mentioned above methods can be used, however here the voltage control has only been considered. Using mathematical modelling two cases have been compared:

 − classical control with external smooth source supplying the commutator [3, 8],
 − classical control with external switching converter supplying the commutator.

The machine was operating during motoring and regenerative braking with energy recuperation to the dc source.

The backgrounds for this paper were previously published in the conference proceedings [7]. However, some information presented there must be corrected with this paper.

## 2. Mathematical model of BLDCM with two 3-phase stator windings

### 2.1. Expressions in natural variables

Main assumptions:
- smooth cylindrical stator,
- cylindrical rotor with surface mounted permanent magnets having the assumed permeability of the air,
- symmetrical, magnetically coupled phase windings, mutually displaced as shown in Figure 1.
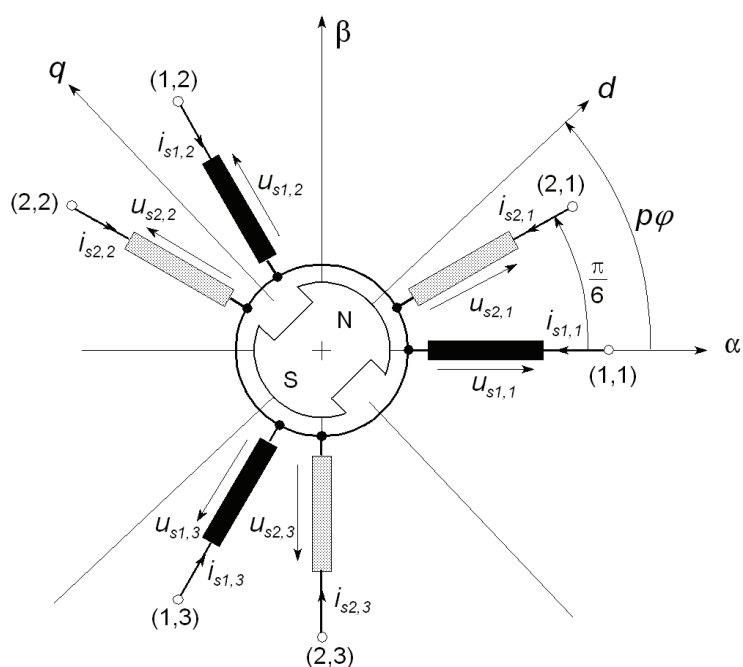


Fig. 1. BLDCM with a double stator winding – schematic diagram

Hence,
- the phase windings have the same resistance $R_s$ and the same leakage inductance $L_{\sigma s}$,
- the self and mutual inductances are described by the formula:

$$M_{i,j} = \frac{2}{3} L_m \cos p(x_i - x_j) = \frac{2}{3} L_m \cos \Delta x_{i,j}, \tag{1}$$

where: $x_i, x_j$ – position angles of stator windings, $L_m$ – so called main inductance. The mutual "electrical" displacements between phase windings take the values:
- $\Delta x_{i,j} = 0°, \pm120°, \pm240°$ for phases belonging to one of the two 3-phase windings,
- $\Delta x_{i,j} = \pm30°, \pm150°, \pm270°$ for phases belonging separately to the first- and the second 3-phase winding.

Voltage equations describing the machine may be written in a matrix form:

$$\left.\begin{aligned}
\mathbf{U_{s1}^I} &= \mathbf{R_{s1}^I}\,\mathbf{I_{s1}^I} + \mathbf{L_{s1}^I}\,\frac{d}{dt}\mathbf{I_{s1}^I} + \mathbf{M_{s12}^I}\,\frac{d}{dt}\mathbf{I_{s2}^I} + \mathbf{E_{f1}^I} \\
\mathbf{U_{s2}^I} &= \mathbf{R_{s2}^I}\,\mathbf{I_{s2}^I} + \mathbf{L_{s2}^I}\,\frac{d}{dt}\mathbf{I_{s2}^I} + \mathbf{M_{s21}^I}\,\frac{d}{dt}\mathbf{I_{s2}^I} + \mathbf{E_{f2}^I}
\end{aligned}\right\}. \tag{2}$$

Vectors and matrices of these equations take the following form presented below.

$$\mathbf{U_{s1}^I} = \begin{bmatrix} u_{s1,1} \\ u_{s1,2} \\ u_{s1,3} \end{bmatrix}; \quad \mathbf{I_{s1}^I} = \begin{bmatrix} i_{s1,1} \\ i_{s1,2} \\ i_{s1,3} \end{bmatrix}; \quad \mathbf{U_{s2}^I} = \begin{bmatrix} u_{s2,1} \\ u_{s2,2} \\ u_{s2,3} \end{bmatrix}; \quad \mathbf{I_{s2}^I} = \begin{bmatrix} i_{s2,1} \\ i_{s2,2} \\ i_{s2,3} \end{bmatrix}, \tag{3}$$

$$\mathbf{R_{s1}^I} = \mathbf{R_{s2}^I} = \begin{bmatrix} R_s & & \\ & R_s & \\ & & R_s \end{bmatrix}, \tag{4}$$

$$\mathbf{L_{s1}^I} = \mathbf{L_{s2}^I} = \frac{2}{3}\begin{bmatrix} \frac{3}{2}L_{\sigma s} + L_m & -\frac{1}{2}L_m & -\frac{1}{2}L_m \\ -\frac{1}{2}L_m & \frac{3}{2}L_{\sigma s} + L_m & -\frac{1}{2}L_m \\ -\frac{1}{2}L_m & -\frac{1}{2}L_m & \frac{3}{2}L_{\sigma s} + L_m \end{bmatrix}, \tag{5}$$

$$\mathbf{M_{s12}^I} = \frac{2}{3}L_m\frac{\sqrt{3}}{2}\begin{bmatrix} 1 & -1 & 0 \\ 0 & 1 & -1 \\ -1 & 0 & 1 \end{bmatrix}; \quad \mathbf{M_{s21}^I} = \mathbf{M_{s12}^{IT}}. \tag{6}$$

The electromotive forces (EMF) have the same form for the both 3-phase winding systems $k = 1, 2$:

$$\mathbf{E_{fk}^I} = \frac{d}{dt}\mathbf{\Psi_{fk}^I} = \frac{\partial\varphi}{\partial t}\frac{\partial}{\partial\varphi}\begin{bmatrix} \psi_{fk,1} \\ \psi_{fk,2} \\ \psi_{fk,3} \end{bmatrix} = \omega\,p\Psi_f\begin{bmatrix} F_{fk,1} \\ F_{fk,2} \\ F_{fk,3} \end{bmatrix} = \omega\,p\,\Psi_f\,\mathbf{F_{fk}^I}, \tag{7}$$

where: $\mathbf{\Psi^I_{f1}}$, $\mathbf{\Psi^I_{f2}}$ – vectors of permanent magnet flux linkages, $\Psi_f$ – magnitude of one phase flux linkage waveform, $\mathbf{F^I_{f1}}$, $\mathbf{F^I_{f2}}$ – vectors of p. u. electromotive forces (EMF) induced in stator phase windings, $\varphi$ – rotor rotation angle, $\omega = d\varphi/dt$ – rotor angular speed, $p$ – the number of pole pairs, superscript $T$ – transposition index. These electromotive forces can be approximated using sinusoidal or non-sinusoidal functions of $\varphi$. The modelled waveforms should be similar to real voltages dependent on shape of permanent magnet poles with respect to the stator winding displacement. Chosen four cases of EMF [1, 13, 18] are described below and shown in Figure 2.

A) Sinusoidal EMF

$$F_{f\,k,i} = -\sin(\varphi_{k,i}),\tag{8}$$

where: $k = 1, 2$ ; $i = 1, 2, 3$,

$$\varphi_{k,i} = \varphi_e - (i-1)\frac{2\pi}{3} - (k-1)\gamma_s\,;\ \gamma_s = \frac{\pi}{6}.$$

The flux linkages

$$\psi_{f\,k,i} = p\Psi_f \int\limits_0^\varphi F_{k,i}(\xi)\,d\xi = \Psi_f \cos(\varphi_{k,i}),\tag{9}$$

$\varphi_e = p\varphi$ – "electrical" angle of rotation, $\xi$ – dummy variable of integration.

B) Non-sinusoidal EMF

$$F_{f\,k,i} = -\frac{1}{2B}\{\arctan[A\sin(\varphi_{k,i}-\frac{\pi}{6})] - \arctan[A\sin(\varphi_{k,i+1}-\frac{\pi}{6})]\},\tag{10}$$

where: $A = 2,...,10$; $B = \arctan(A)$; $k = 1,2$ ; $i = 1,2,3$.

C) Trapezoidal EMF (based on formulae presented in [9])

$$F_{f\,k,i} = -\frac{1}{2\alpha M}\{\arcsin[\sin(\varphi_{k,i}+\beta_M)] + \arcsin[\sin(\varphi_{k,i}-\beta_M)]\},\tag{11}$$

where:

$$\alpha_M = \frac{\pi}{6},\ \beta_M = \frac{\pi}{2} - \alpha_M.$$

D) Near-trapezoidal EMF

The Fourier series expansion of the trapezoidal function of magnitude 1 gives:

$$F_{f\,k,i} = -\frac{4}{\pi}\frac{1}{\alpha_M}(\sin\alpha_M\sin\varphi_{k,i} + \frac{1}{9}\sin 3\alpha_M\sin 3\varphi_{k,i} + \frac{1}{25}\sin 5\alpha_M\sin 5\varphi_{k,i} + ...$$

$$...+ \frac{1}{n^2}\sin n\alpha_M\sin n\varphi_{k,i} + \frac{1}{n^2}\sin n\alpha_M\sin n\varphi_{k,i}).\tag{12}$$

For $\alpha_M = \pi/6$ and $n_{max} = 5$

$$F_{f\,k,i} = -\frac{24}{\pi^2}\left(\frac{1}{2}\sin\varphi_{k,i} + \frac{1}{9}\sin 3\varphi_{k,i} + \frac{1}{50}\sin 5\varphi_{k,i}\right) =$$
$$= -(f_1\sin\varphi_{k,i} + f_3\sin 3\varphi_{k,i} + f_5\sin 5\varphi_{k,i}), \tag{13}$$

$$\psi_{f\,k,i} = p\Psi_f\int_0^\varphi F_{i,k}(\xi)\,d\xi = \Psi_f\,\frac{24}{\pi^2}[\frac{1}{2}\cos\varphi_{k,i} + \frac{1}{27}\cos 3\varphi_{k,i} + \frac{1}{250}\cos 5\varphi_{k,i}] =$$
$$= \Psi_f[f_1\cos\varphi_{k,i} + \frac{1}{3}f_3\cos 3\varphi_{k,i} + \frac{1}{5}f_5\cos 5\varphi_{k,i}]. \tag{14}$$

Electromagnetic torque is given by the expression:

$$T_e = \mathbf{I}_{s1}^{IT}\frac{\partial}{\partial\varphi}\boldsymbol{\Psi}_{f1}^{I} + \mathbf{I}_{s2}^{IT}\frac{\partial}{\partial\varphi}\boldsymbol{\Psi}_{f2}^{I} = p\Psi_f\left\{\mathbf{I}_{s1}^{IT}\mathbf{F}_{f1}^{I} + \mathbf{I}_{s2}^{IT}\mathbf{F}_{f2}^{I}\right\} \tag{15}$$
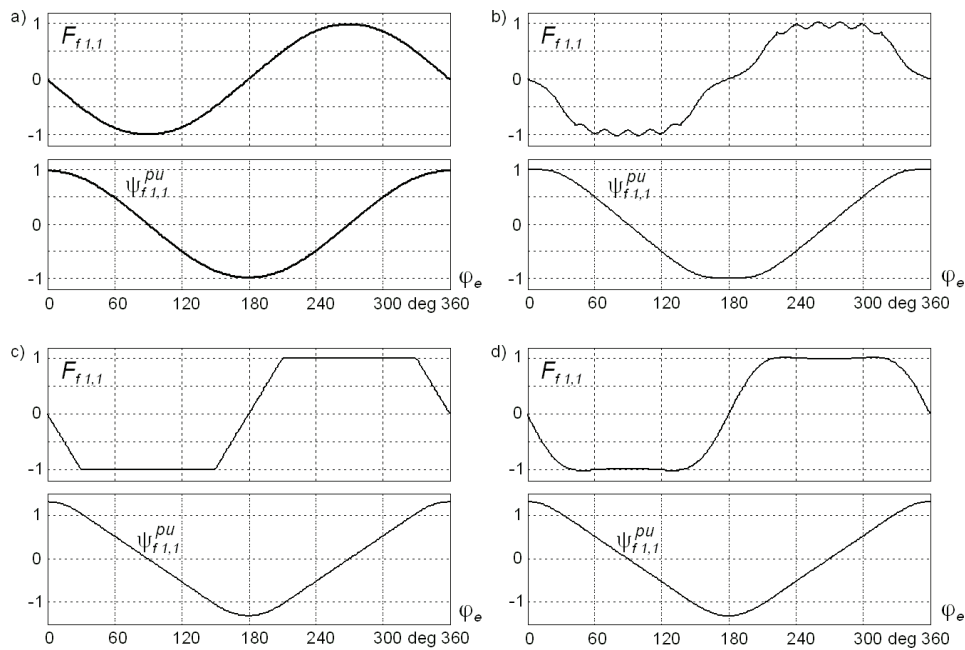


Fig. 2. Examples of EMF and magnetic flux waveforms: a) sinusoidal, b) non-sinusoidal with superimposed influence of slotting, c) pure trapezoidal, d) near trapezoidal

## 2.2. Expressions in symmetrical components

Transformation to symmetrical components can be performed for both the 3-phase windings separately. Introducing the below transformation matrices $\mathbf{S}$ and $\mathbf{S}^{-1}$

$$\mathbf{S} = C \begin{bmatrix} 1 & 1 & 1 \\ 1 & \underline{a} & \underline{a}^2 \\ 1 & \underline{a}^2 & \underline{a} \end{bmatrix} = C \, \mathbf{S_0} \; ; \; \mathbf{S}^{-1} = \frac{1}{3C} \mathbf{S_0^*} \; ; \; \underline{a} = e^{j2\pi/3} = -\frac{1}{2} + j\frac{\sqrt{3}}{2} \tag{16}$$

into voltage Equations (2) yields

$$\mathbf{U_{s1}^{II}} = \mathbf{SU_{s1}^{I}} = \mathbf{SR_{s1}^{I}S^{-1}SI_{s1}^{I}} + \mathbf{SL_{s1}^{I}S^{-1}S}\frac{d}{dt}\mathbf{I_{s1}^{I}} + \mathbf{SM_{s12}^{I}S^{-1}S}\frac{d}{dt}\mathbf{I_{s2}^{I}} + \mathbf{SE_{f1}^{I}}, \tag{17}$$

$$\mathbf{U_{s2}^{II}} = \mathbf{SU_{s2}^{I}} = \mathbf{SR_{s1}^{I}S^{-1}SI_{s2}^{I}} + \mathbf{SL_{s2}^{I}S^{-1}S}\frac{d}{dt}\mathbf{I_{s2}^{I}} + \mathbf{SM_{s12}^{IT}S^{-1}S}\frac{d}{dt}\mathbf{I_{s1}^{I}} + \mathbf{SE_{f2}^{I}}, \tag{18}$$

where: * – conjugation index.

For electrical drives this is profitable to assume $C = 2/3$, whereas for power invariant transformation of 3-phase systems $C = 1/\sqrt{3}$. Vectors of symmetrical components for voltages ($\mathbf{X} = \mathbf{U}$), currents ($\mathbf{X} = \mathbf{I}$) and electromotive forces ($\mathbf{X} = \mathbf{F}$) take the generic form

$$\mathbf{X_{sk}^{II}} = \mathbf{SX_{sk}^{I}} = \begin{bmatrix} x_{sk}^{(0)} \\ \underline{x}_{sk}^{(1)} \\ \underline{x}_{sk}^{(2)} \end{bmatrix} = \begin{bmatrix} x_{s0k} \\ x_{s\alpha k} + jx_{s\beta k} \\ x_{s\alpha k} - jx_{s\beta k} \end{bmatrix}_{k=1,\,2}, \tag{19}$$

where $x$ must be substituted with $u$, $i$, $F$.

After transformation the matrices of resistances and winding inductances become diagonal, whereas the last two terms of Equations (17) and (18) are:

$$\mathbf{SM_{s12}^{I}S^{-1}} = \sqrt{3}L_m \mathrm{diag}[0, \, e^{j\frac{\pi}{6}}, e^{-j\frac{\pi}{6}}], \tag{20}$$

$$\mathbf{SM_{s12}^{IT}S^{-1}} = \sqrt{3}L_m \mathrm{diag}[0, \, e^{-j\frac{\pi}{6}}, e^{+j\frac{\pi}{6}}], \tag{21}$$

$$\mathbf{SE_{fk}^{I}} = \omega p \Psi_f \, \mathbf{SF_{fk}^{I}} = \omega p \Psi_f \begin{bmatrix} F_{fk}^{(0)} \\ F_{fk}^{(1)} \\ F_{fk}^{(2)} \end{bmatrix}. \tag{22}$$

### 2.3. Expressions in common reference frame

All vectors can be expressed in the same reference frame $\alpha_1$-$\beta_1$, attached to the first 3-phase winding, denoted now $\alpha$-$\beta$:

$$\underline{x}_{s1} = \underline{x}_{s1}^{(1)} = x_{s1\alpha} + jx_{s1\beta}, \tag{23}$$

where: $x_{s1\alpha} = x_{s\alpha 1}$, $x_{s1\beta} = x_{s\beta 1}$.

$$\underline{x}_{s2} = \underline{x}_{s2}^{(1)} e^{j\frac{\pi}{6}} = (x_{s\alpha 2} + jx_{s\beta 2})(\frac{\sqrt{3}}{2} + j\frac{1}{2}) = x_{s2\alpha} + jx_{s2\beta}. \tag{24}$$

For star connected windings the differential equations for zero-sequence symmetrical components must be omitted. Hence, the voltage equations take the form:

$$\left.\begin{aligned}
\underline{u}_{s1} &= R_s \underline{i}_{s1} + L_s \frac{d}{dt}\underline{i}_{s1} + L_m \frac{d}{dt}\underline{i}_{s2} + p\omega\Psi_f \underline{F}_{f1} \\
\underline{u}_{s2} &= R_s \underline{i}_{s2} + L_s \frac{d}{dt}\underline{i}_{s2} + L_m \frac{d}{dt}\underline{i}_{s1} + p\omega\Psi_f \underline{F}_{f2}
\end{aligned}\right\}, \tag{25}$$

where: $L_s = L_{\sigma s} + L_m$.

Electromagnetic torque after transformation:

$$T_e = p\,\Psi_f \left\{ \mathbf{I_{s1}^{IT} S^{-1} S F_{f1}^{I}} + \mathbf{I_{s2}^{IT} S^{-1} S F_{f2}^{I}} \right\} = \frac{1}{3C^2} p\Psi_f \left\{ \mathbf{I_{s1}^{II*} F_{f1}^{II}} + \mathbf{I_{s2}^{II*} F_{f2}^{II}} \right\} =$$

$$= \frac{2}{3C^2} p\,\Psi_f \operatorname{Re}\left\{ \underline{i}_{s1}^* \underline{F}_{f1} + \underline{i}_{s2}^* \underline{F}_{f2} \right\} = \tag{26}$$

$$= \frac{2}{3C^2} p\,\Psi_f (i_{s\alpha1}F_{f\alpha1} + i_{s\beta1}F_{f\beta1} + i_{s\alpha2}F_{f\alpha2} + i_{s\beta2}F_{f\beta2}) =$$

$$= \frac{2}{3C^2} p\,\Psi_f (i_{s1\alpha}F_{f1\alpha} + i_{s1\beta}F_{f1\beta} + i_{s2\alpha}F_{f2\alpha} + i_{s2\beta}F_{f2\beta}).$$

### 2.4. Expressions with EMF harmonics

Incorporating (13) in the above equations and substituting $C = 2/3$ yields

$$\left.\begin{aligned}
\underline{u}_{s1} &= R_s \underline{i}_{s1} + L_s \frac{d}{dt}\underline{i}_{s1} + L_m \frac{d}{dt}\underline{i}_{s2} + jp\omega\Psi_f (f_1 e^{jp\varphi} - f_5 e^{-j5p\varphi}) \\
\underline{u}_{s2} &= R_s \underline{i}_{s2} + L_s \frac{d}{dt}\underline{i}_{s2} + L_m \frac{d}{dt}\underline{i}_{s1} + jp\omega\Psi_f (f_1 e^{jp\varphi} + f_5 e^{-j5p\varphi})
\end{aligned}\right\}. \tag{27}$$

The zero sequence voltages induced in phase windings:

$$\left.\begin{aligned}
u_{s1}^{(0)} &= -2\omega p\,\Psi_f f_3 \sin 3p\varphi \\
u_{s2}^{(0)} &= 2\omega p\,\Psi_f f_3 \cos 3p\varphi
\end{aligned}\right\}. \tag{28}$$

Electromagnetic torque

$$T_e = -j\frac{3}{2} p\,\Psi_f \{ \underline{i}_{s1}^* (f_1 e^{jp\varphi} - f_5 e^{-j5p\varphi}) - \underline{i}_{s1}(f_1 e^{-jp\varphi} - f_5 e^{+j5p\varphi}) +$$

$$+ \underline{i}_{s2}^* (f_1 e^{jp\varphi} + f_5 e^{-j5p\varphi}) - \underline{i}_{s2}(f_1 e^{-jp\varphi} + f_5 e^{+j5p\varphi}) \} = \tag{29}$$

$$= \frac{3}{2} p\,\Psi_f \operatorname{Im}\{ \underline{i}_{s1}^* (f_1 e^{jp\varphi} - f_5 e^{-j5p\varphi}) + \underline{i}_{s2}^* (f_1 e^{jp\varphi} + f_5 e^{-j5p\varphi}) \}.$$

Transformation to the rotor reference frame *d-q* yields

$$\underline{u}_{s1}^{dq} = \underline{u}_{s1} e^{-jp\varphi} = u_{s1d} + ju_{s1q}$$

$$u_{s2}^{dq} = \underline{u}_{s2} e^{-jp\varphi} = u_{s2d} + ju_{s2q}$$

$$\underline{i}_{s1}^{dq} = \underline{i}_{s1} e^{-jp\varphi} = i_{s1d} + ji_{s1q}$$

$$\underline{i}_{s2}^{dq} = \underline{i}_{s2} e^{-jp\varphi} = i_{s2d} + ji_{s2q},$$

(30)

$$T_e = \frac{3}{2} p\Psi_f \, \mathrm{Im}\{\underline{i}_{s1}^{dq*}(f_1 - f_5 e^{-j6p\varphi}) + \underline{i}_{s2}^{dq*}(f_1 + f_5 e^{-j6p\varphi})\}. \tag{31}$$

Considering more harmonics of EMF in Fourier series (13) the expression describing electromagnetic torque for $n = 1, 3, 5, 7, 9, 11, 13, ...$ and the voltage equations (27) assume a generic forms:

$$T_e = \frac{3}{2} p\Psi_f \, \mathrm{Im} \, \{\underline{i}_{s1}^{dq*}(f_1 - f_5 e^{-j6p\varphi} + f_7 e^{j6p\varphi} - f_{11}e^{-j12p\varphi} + f_{13}e^{j12p\varphi} - ...) +$$

(32)

$$+ \underline{i}_{s2}^{dq*}(f_1 + f_5 e^{-j6p\varphi} - f_7 e^{j6p\varphi} + f_{11}e^{-j12p\varphi} - f_{13}e^{j12p\varphi} + ...)\},$$

$$\left.\begin{array}{l}
\underline{u}_{s1}^{dq} = R_s \underline{i}_{s1}^{dq} + L_s \dfrac{d}{dt}\underline{i}_{s1}^{dq} + L_m \dfrac{d}{dt}\underline{i}_{s2}^{dq} + jp\omega[L_s \underline{i}_{s1}^{dq} + L_m \underline{i}_{s2}^{dq} + \\[2mm]
+ \Psi_f (f_1 - f_5 e^{-j6p\varphi} + f_7 e^{j6p\varphi} - f_{11}e^{-j12p\varphi} + f_{13}e^{j12p\varphi} - ...)] \\[4mm]
\underline{u}_{s2}^{dq} = R_s \underline{i}_{s2}^{dq} + L_s \frac{d}{dt}\underline{i}_{s2}^{dq} + L_m \frac{d}{dt}\underline{i}_{s1}^{dq} + jp\omega[L_s \underline{i}_{s2}^{dq} + L_m \underline{i}_{s1}^{dq} + \\[2mm]
+ \Psi_f (f_1 + f_5 e^{-j6p\varphi} - f_7 e^{j6p\varphi} + f_{11}e^{-j12p\varphi} - f_{13}e^{j12p\varphi} + ...)]
\end{array}\right\}. \tag{33}$$

Assuming $\underline{i}_{s1}^{dq} = \underline{i}_{s2}^{dq} = \underline{i}_{s}^{dq}$ (e. g. due to some control method) the alternating components, dependent on multiples $6p$ of the rotation angle $\varphi$, compensate mutually in expression (32) for electromagnetic torque. So, the torque becomes twice as the produced by one 3-phase winding

$$T_e = \frac{3}{2} p \, \Psi_f f_1 \, (i_{sq1} + i_{sq2}) = 3p \, \Psi_f f_1 \, i_{sq}. \tag{34}$$

For ideally trapezoidal EMFs induced in phases the zero sequence voltages are triangle waveforms containing alternating components that are multiples of $3p\varphi$:

$$\left.\begin{array}{l}
u_{s1}^{(0)} = -2\omega p \, \Psi_f (f_3 \sin 3p\varphi + f_9 \sin 9p\varphi + ...) \\[2mm]
u_{s2}^{(0)} = 2\omega p \, \Psi_f (f_3 \cos 3p\varphi + f_9 \cos 9p\varphi + ...)
\end{array}\right\} \tag{35}$$

The dominant is third harmonic as in (28), whereas the remaining higher harmonics distort these harmonic voltages in the greater degree the closer to trapezoidal are induced EMFs. These components can be used for sensor-less control of the motor. The component $u_{s2}^{(0)}$ is suitable for control currents in winding 1, whereas $u_{s1}^{(0)}$ for control currents in winding 2. So, there is no necessity to integrate the zero sequence voltages to obtain zero crossing instants at

which the phase currents are turned on or off as it was proposed in [2, 15, 16] for 3-phase permanent magnet machines.
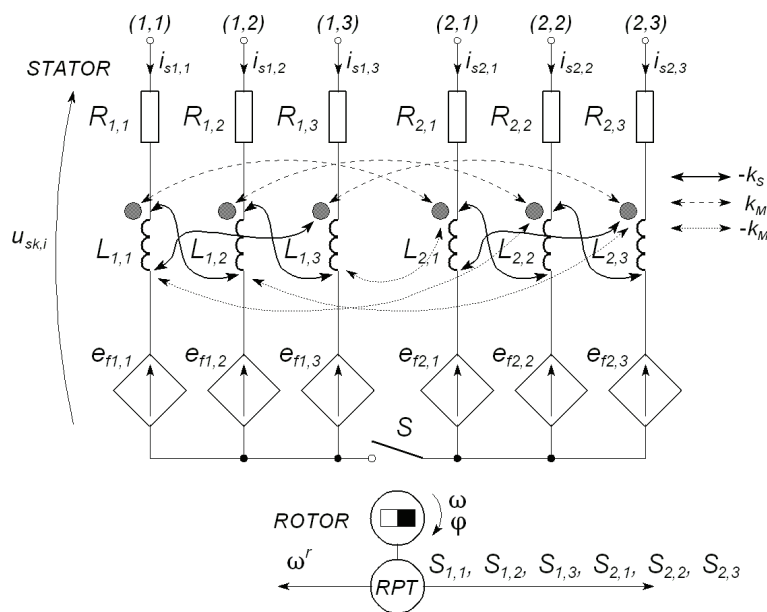


Fig. 3. Equivalent circuit of the permanent magnet machine with a double stator winding designed for circuit oriented computer simulators (for BLDCM)

## 3. Analysis of motor operation

### 3.1. Parameters of the mathematical model

Equivalent circuit of the permanent magnet machine, co-operating with the electronic commutator as the BLDCM, suitable for circuit oriented simulators (Spice family programs or SimPowerSystems of Simulink, etc.), results directly from equations (2) and the defined parameters. This is shown in Figure 3. The following parameters were taken there: $R_{k,i} = R_s = 1.1\ \Omega$, $L_{k,i} = L_{\sigma s} + 2/3 L_m = 5$ mH, $\Psi_f = 0.52$ Wb, $p = 3$, $e_{k,i} = p\omega\Psi_f F_{k,i}$, moment of inertia $J = 0.5$ kgm$^2$ and the loading torque $T_L = D_L\omega$ ($D_L = 0.15$ Nms). Magnetic coupling factors

$$0 \le k_S = \frac{1}{3\sigma_s + 2} < 0.5, \quad k_M = \frac{\sqrt{3}}{2}k_S \quad (\sigma_s = \frac{L_{\sigma s}}{L_m}).$$

### 3.2. Analysis of basic operation

The permanent magnet machine is connected with the electronic commutator, as it has been shown in Figure 4, creating BLDCM.
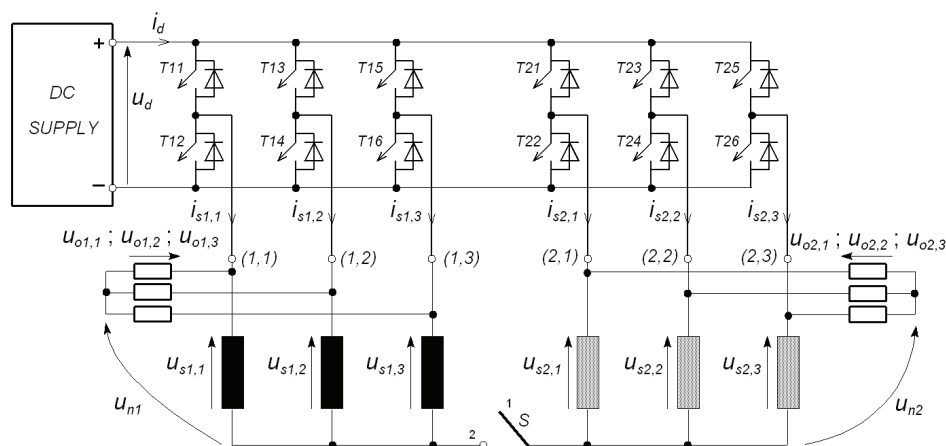
Fig. 4. Connection of the permanent magnet machine with the electronic commutator

The are considered two cases: separate supply, for switch *S* in position 1, when each 3-phase winding is supplied separately [12] and the common supply, for *S* in position 2, when mutual influence due to galvanic connection between the windings occurs. The magnetic coupling between the phases depends on the machine design and causes mutual influence at the both separate- and common supply. Alternatively, these two 3-phase commutators could be connected in series carrying the same DC link supply current as it was proposed in [10, 12]. In this paper the motor operation was analysed for external converter supplying the commutator, whereas the commutator was triggered due to signals $S_{k,i}$ produced for each half-bridge by the rotor position transducer (*RPT* in Fig. 3). Since the commutator is composed of single-direction controlled switches these signals must be multiplied by signal $S_{ua} = \text{sgn}(u_a^c)$ determining the sign of demanded armature voltage signal $u_a^c$ causing reverse of speed. In the result the signals $Q_{k,i} = S_{ua}S_{k,i}$ trigger the commutator switches. If $Q_{k,i} = 1$ then the "positive" switch of the respective half-bridge is turned on, and for $Q_{k,i} = -1$ the "negative" switch is turned on. It has been shown schematically in Figure 5a.

To analyse the machine behaviour the steady state operation of the motor was simulated at a constant speed $\omega = 70$ rad/s, for the smooth, regulated supply in the commutator input (*DC SUPPLY*). Results of calculations are presented in Figure 6. The first analysed case concerns the operation at lack of magnetic coupling and separate supply of the both 3-phase windings (switch *S* in position 1, Fig. 6a). For the second case the magnetic coupling was taken into account (Fig. 6b) and for the third one the machine had the magnetic coupling and the commutator was supplied with a common regulated DC source (switch *S* in position 2, Fig. 6c).

The obtained results show that separate supply assures the same phase current waveforms in the both 3-phase winding ($i_{s1,1}, i_{s2,1}$) displaced mutually with 30°. The electromagnetic torque waveforms $T_{e1}, T_{e2}$ produced by these windings and the common rotor have also the same displaced shapes and values. Thus, the machine operation can be considered as symmetrical. The influence of magnetic coupling appears mainly in current and torque waveforms

(Figs. 6a and 6b). A significant difference appears when the stator windings are supplied in the common way (Fig. 6c). The currents for respective phases of the both 3-phase windings are different.
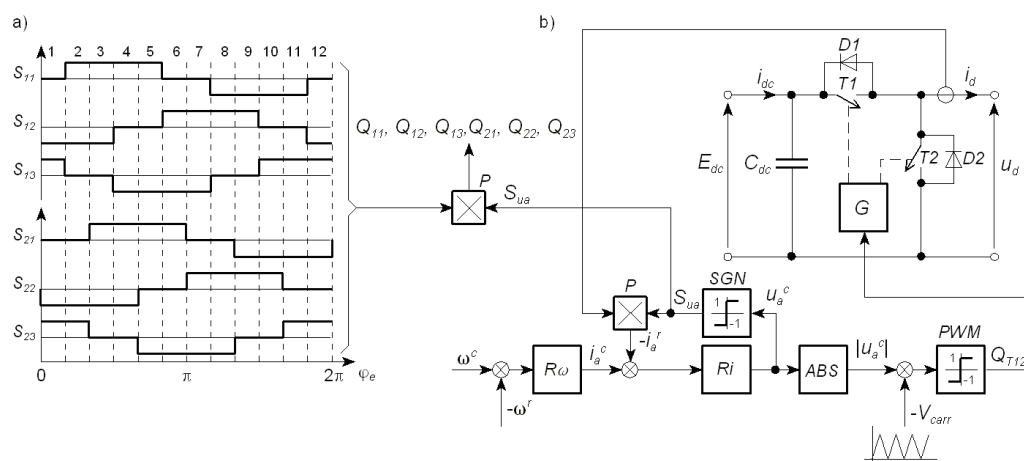


Fig. 5. Principle of BLDCM control: a) triggering of commutator half-bridges,
b) automatic control due to the external converter

The produced torque components $T_{e1}, T_{e2}$ have also visible differences, though the effect of 12 pulse total torque waveform $T_e = T_{e1} + T_{e2}$ also appears as for the two previous cases. The measured neutral voltages $u_{n1}, u_{n2}$ have triangle shapes, though distorted in a greater degree than those in Figures 6a and 6b. According to (19) the zero sequence symmetrical components $u_{sk}^{(0)} = Cu_{nk}$ (35) can be determined from these neutral voltages. The influence on difference of phase voltage waveforms $u_{s1,1}, u_{s2,1}$ is not important. These asymmetries are caused by mutual current connections through switched phases belonging to these both 3-phase winding systems. This is obvious from the triggering pulse waveforms presented in Figure 5a.

### 3.3. Automatic control

For speed control of the motor the worst case for common supply was analysed. For automatic speed control the structure of control system presented in Figure 5b was chosen. The two-quadrant switching converter supplying the commutator was controlled with absolute value of voltage signal $u_a^c$ of current controller (*Ri*) output. The pulse width modulation (PWM) was used with the saw-tooth carrier $V_{carr}$ of frequency 1 kHz. The speed controller (*Rω*) produces the output signal $i_a^c$ of demanded armature current $i_a = S_{ua}i_d$. This current is equivalent to the armature current of conventional commutator machine.

The desired reference speed signal $\omega^c$ was settled in the stepper way for the motor starting and reverse. Results of simulation are shown in Figure 7. There are presented: speed $\omega$ and electromagnetic torque $T_e$, armature current $i_{a0}$ filtered with the low pass RC filter of time constant $RC = 1$ ms, phase currents $i_{s1,1}$, $i_{s2,1}$, phase voltages $u_{s1,1}$, $u_{s2,1}$ and neutral voltages $u_{n1}$, $u_{n2}$ measured between the pseudo neutral points of resistors and the star point of the
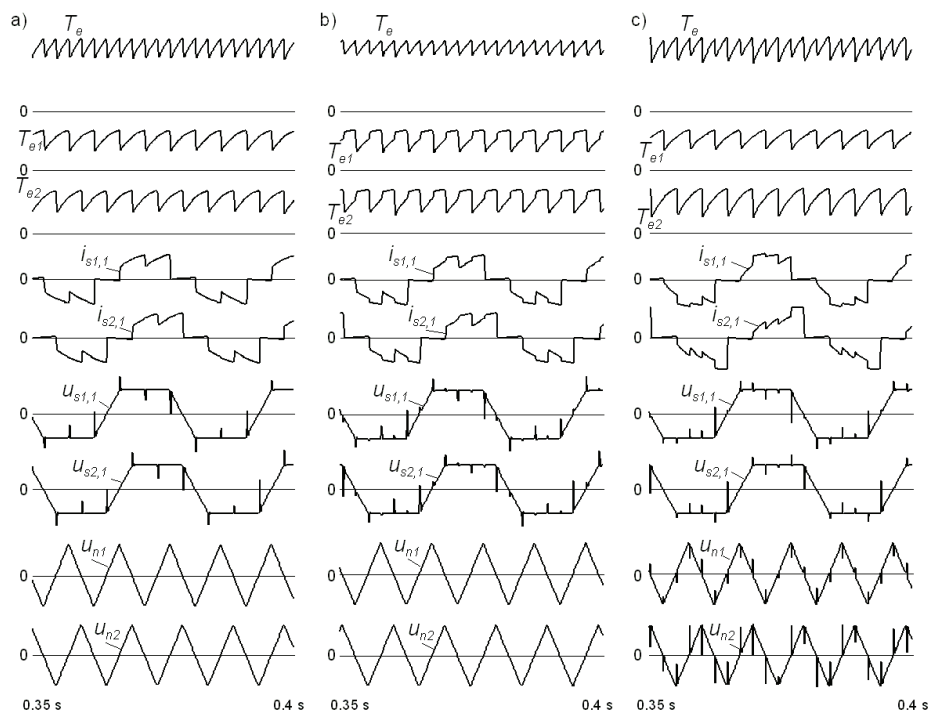
Fig. 6. Steady state waveform of BLDCM supplied with smooth regulated voltage in the commutator input: a) for separate supply and lack of magnetic coupling between phase windings, b) for separate supply and considered magnetic coupling, c) for common supply of commutator and the machine with magnetic coupling

windings (Fig. 4). Additionally the filtered neutral voltages $u_{n10}$, $u_{n20}$ ($RC = 0.5$ ms) are shown there, since the neutral voltages $u_{n1}$, $u_{n2}$ are strongly distorted from the triangle shape with PWM effects and then they could not be used for the mentioned earlier sensor-less control. The drive operates properly and the armature current $i_a$ is the measure of the motor electromagnetic torque $T_e = 3/2\,p\Psi_f\,i_a$ .

## 4. Conclusions

Both the torque components $T_{e1}$, $T_{e2}$ produced by the first- and the second 3-phase windings cause that the resultant electromagnetic torque $T_e$ has two times lower amplitude of alternating component (Fig. 6), and two times greater frequency than the motor with a single 3-phase winding. It was expected from the presented above theory, where the EMF harmonics were reduced mutually in the expression for electromagnetic torque. At PWM control this phenomenon appears as well. This has been observed for operation at separated supply (switch *S* in Fig. 4 opened) and the operation at common supply (switch *S* closed). So, this motor influences the mechanical transmission system in a less disadvantageous degree than the 3-phase one.
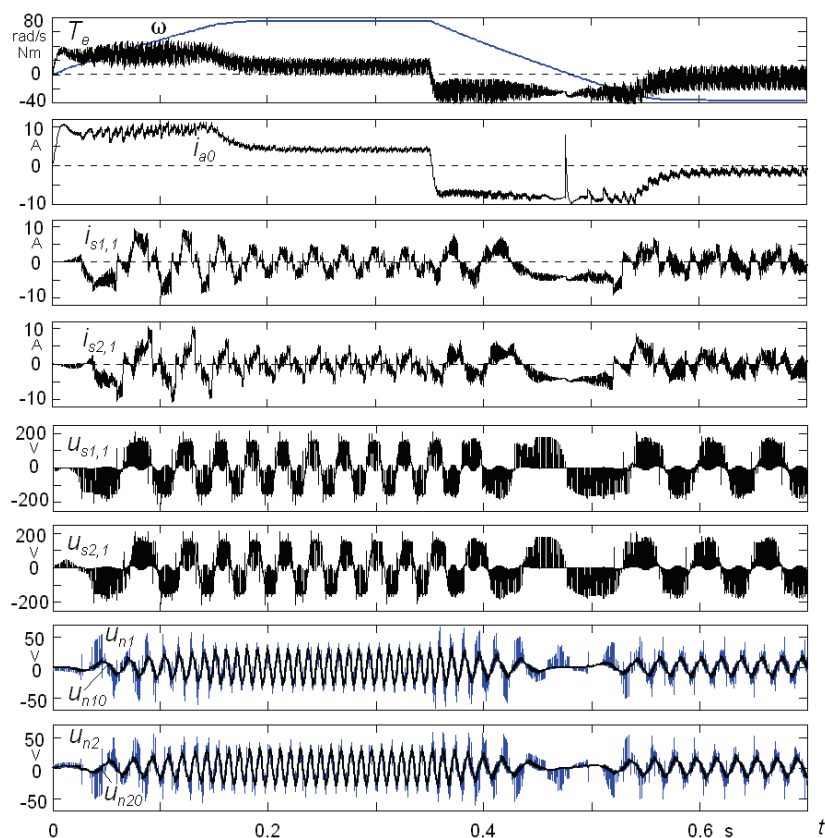
Fig. 7. Waveforms for automatic control of drive with a double 3-phase BLDCM

As for all multiphase motors the transistors of the commutator can be dimensioned for a lower current at the given power. However, in case of one 3-phase system damaged (commutator or winding damage) the motor can continue operation with two times lower power utilising the second 3-phase system after turning off the first one. For some applications or a manufacturing process this can be indispensable.

The measured signals of neutral voltages $u_{n1}$, $u_{n2}$ (zero symmetrical components) can be used for sensor-less control applying the technique described in [16] (page 144) for the 3-phase machine. In contradistinction to the method described there the voltages $u_{n1}$, $u_{n2}$ need not be integrated to obtain two signals displaced mutually by 90 degrees. Simply, the zero sequence voltage produced by one 3-phase winding is used for triggering the commutator supplying the second winding and vice versa. The triggering signals appear immediately and this method seems less absorbing then this based on back EMFs determination. This could be profitable for current controlled high-speed motors.

The vector form of presented motor equations can be used for vector control of this motor and the motor model presented in the form of equivalent circuit (Fig. 4) can be extended and

supplemented with phenomenon of cogging torques. The theory presented in [18] could be used then.

## References

[1] Ciurys M., Dudzikowski I., *Modelling of BLDC motor incorporating an actual waveform of back EMF* (in Polish: *Modelowanie silnika bezszczotkowego z uwzględnieniem rzeczywistego przebiegu siły elektromotorycznej*). Sc. Papers of the Inst. of El. Machines, Drives and Metrology 62/28, Wroclaw Univ. of Tech., Wrocław (2008).

[2] Dae-Kyu Jang, Jung-Hwan Chang, Gun-Hee Jang, *Back EMF Design of an AFPM Motor using PCB Winding by Quasi 3D Space Harmonic Analysis Method.* Journal of Electrical Engineering & Technology 7(5): 730-735 (2012).

[3] Domoracki A., Krykowski K., *BLDC motors – classical control methods* (in Polish: *Silniki bldc – klasyczne metody sterowania*). Zeszyty Problemowe BOBRME – Maszyny Elektryczne 72: 155-159 (2005).

[4] Drozdowski P., *Control properties of the PM brushless DC motor with rectangular and stepwise currents*. Proc. of 3rd Int. Conf. Drives and Supply Systems for Modern Electric Traction, pp. 98-103 Warsaw (1997).

[5] Drozdowski P., Jagiełło A., *The commutation process modelled by the serraphile functions and its influence on controlled brushless dc machines*. Sc. Bull. of Lodz Techn. Univ. Elektryka, 91(788): 39-44, Łódź (1998).

[6] Drozdowski P., Szular Z., *Voltage control of permanent magnet synchronous generator using a static converter* (in Polish: *Sterowanie napięcia wyjściowego generatora synchronicznego wzbudzanego magnesami trwałymi za pomocą układu przekształtnikowego*). Sc. Letters of Silesian Univ. of Tech. Elektryka 177: 203-210, Gliwice (2001).

[7] Drozdowski P., *Modelling of BLDCM with Asymmetrical Double Stator Winding and Back EMF Harmonics*. KOMEL Transactions 104(4): 111-116, Katowice (2014).

[8] Glinka T., *Permanent magnet electrical machines* (book in Polish: *Maszyny elektryczne wzbudzane magnesami trwałymi*). Gliwice (Poland), Silesian Univ. of Tech. (2002).

[9] Jagiełło A., *The transformations not allowed for integration in the theory of electrical machines* (in Polish: *Przekształcenia niecałkowalne w teorii maszyn elektrycznych*). PWN Warszawa (2002).

[10] Jagiełło A., *Brushless DC machine based on the 2x3 phase synchronous motor* (in Polish: *Bezszczotkowa maszyna prądu stałego zbudowana na bazie silnika synchronicznego 2x3 fazowego*). Monograph 450, Electrical and Comp. Eng., Cracow Univ. of Tech., pp. 151-166, Kraków (2014).

[11] José Carlos Gamazo-Real, Ernesto Vázquez-Sánchez, Jaime Gómez-Gil., *Position and Speed Control of Brushless DC Motors Using Sensorless Techniques and Application Trends.* Sensors 2010, 10, www.mdpi.com/journal/sensors, pp. 6901-6947 (2010).

[12] Kallio S., *Modeling and parameter estimation of double-star permanent magnet synchronous machines*. Doctoral Thesis, Lappeenranta University of Technology, Lappeenranta (2014).

[13] Krykowski K., Hetmańczyk J., Gałuszkiewicz Z., Miksiwicz R., *Computer analysis of high-speed PMBLDC motor properties*. Int. Journ. for Comp. and Math. in Electrical and Electronic Eng. COMPEL 30(3): 941-956 (2011).

[14] Nezli L., Elbar M., Naas B., *Direct Torque Control of Double Star Synchronous Machine*. International Journal of Recent Trends in Engineering 2(5): 336-340 (2009).

[15] Shen J.X., Zhu Z.Q., Howe D., *Sensorless Flux-Weakening Control of Permanent-Magnet Brushless Machines Using Third Harmonic Back EMF*. IEEE Transactions on Industry Applications 40(6): 1629 (2004).

[16] Vas P., *Sensorless vector and direct torque control*. Oxford Univ. Press (1998).

[17] Wach P., *Dynamics and control of electrical drives*. Springer (2011).

[18] Węgiel T., *Space harmonics interaction in permanent magnet generators*. Monograph 447. Electrical and Comp. Eng., Cracow Univ. of Technology, Kraków (2013).

[19] Zawirski K., *Control of permanent magnet synchronous motor* (in Polish: *Sterowanie silnikiem synchronicznym o magnesach trwałych*). Poznań, Wyd. Pol. Pozn. (2005).